

POINT SPREAD FUNCTION STUDY OF X-RAY PINHOLE CAMERA IN SSRF*

Zhichu Chen[†], Yongbin Leng[‡], Jie Chen, Guoqing Huang
Shanghai Synchrotron Radiation Facility and Shanghai Institute of Applied Physics,
Chinese Academy of Sciences, Shanghai, China

Abstract

An X-ray pinhole camera that has been used to present the transverse beam size with an intuitive grasp of the distribution of the beam radiation was installed on one beam-line of the storage ring in Shanghai Synchrotron Radiation Facility (SSRF). The real beam size however is a function of the image size of the CCD camera and the point spread function (PSF) of the system. The PSF was calculated but poorly tested. This article will present the measurement of the PSF with a series of beam based experiments and the consistency with the theoretical beam size.

INTRODUCTION

Emittance is the property of the charged beam and a measure for the consistency in position-momentum phase space. The invariability of the emittance due to Liouville's theorem makes it a good estimate of the performance of the particle accelerator. The emittance can be derived by using the following formula [1]:

$$\sigma_i^2 = \beta_i \epsilon_i + (\eta_i \sigma_i)^2, \quad (1)$$

where ϵ_i is the beam emittance, σ_i is the transverse size of the beam, β_i , ϵ_i and η_i are the Twiss parameters which has already been calculated.

To measure the transverse sizes, an X-ray pinhole camera was installed on a beam line of the storage ring of SSRF [2]. The layout of the whole system is shown in Fig. 1. The X-ray would be filtered by the Al window and the staircase Cu attenuator before it passes through the pinhole. The final image is a combination of the photon image, the diffraction in the pinhole, the spacial effect of the X-ray screen and the quantization of the CCD, etc. A rough estimate (the Al window and the Cu filter were only regarded as high-pass filters) of the size of the image can be written as:

$$\begin{aligned} \sigma_{\text{result}}^2 &= \sigma_{\text{photon}}^2 \\ &+ \sigma_{\text{diff}}^2 + \sigma_{\text{aper}}^2 \\ &+ \sigma_{\text{scr}}^2 + \sigma_{\text{mirror}}^2 + \sigma_{\text{lens}}^2 + \sigma_{\text{CCD}}^2, \end{aligned} \quad (2)$$

where σ_{result} is the size of the final image, σ_{photon} the size of the source, σ_{diff} the effect of the pinhole diffraction, σ_{aper} the effect of the pinhole geometry, σ_{scr} PSF of

the phosphor screen, σ_{mirror} distortion in the mirror, σ_{lens} deformation in the lens and σ_{CCD} the digitalization in the CCD.

The analytic PSF of the geometrical and diffraction components of the pinhole can easily be derived [3, 1]:

$$\sigma_{\text{diff}} = \frac{\sqrt{12} \lambda_3 D}{4\pi A}, \quad (3)$$

$$\sigma_{\text{aper}} = \frac{A}{\sqrt{12}} \frac{D+d}{d}, \quad (4)$$

where λ_3 , A , D and d are shown in Fig. 1. The pinhole is actually an array of pinholes that the transverse dimension can be flexibly switched.

The PSF of the imaging system including the screen, the mirror, the lens and the CCD camera is hard to be calculated. The idea of calibrating the total PSF $\sigma_{\text{scr}}^2 + \sigma_{\text{mirror}}^2 + \sigma_{\text{lens}}^2 + \sigma_{\text{CCD}}^2$ of the system has already been discussed in [1]. The Ce³⁺-doped Y₃Al₅O₁₂ crystal (Ce:YAG or YAG:Ce) was chosen to be the phosphor in SSRF due to its short decay time and high producing capacity in visible region [4].

The gain or the exposure time of the CCD camera may need some adjustments according to different machine statuses from time to time. The PSF of the CCD might not be retained when these parameters are changing. The exposure time was decided to be fixed to stabilize the following effects in the CCD camera:

- the possible temporal nonlinearity of the device;
- the influence of the transverse oscillations of the beam.

A calibration is then needed to determine the PSF of the whole imaging system by changing the critical wavelengths of the filtered X-ray and the gain settings of the CCD after removing the pinhole component.

SPECTRUM CALCULATION

The critical wavelength is needed to get the PSFs of the pinhole as shown in Eqs. (3) and (4). The incredible software XOP¹ from ESRF was used in this procedure and the high-pass Cu filter behaves as expected.

The critical wavelength may have nothing to do with the PSF of the YAG screen, [4] but it's a necessity for choosing the size of the aperture of the pinhole and estimating its PSF.

¹<http://www.esrf.eu/UsersAndScience/Experiments/TBS/SciSoft/xop2.3/>

*Work supported by National Natural Science Foundation of China (11075198)

[†]chenzhichu@sinap.ac.cn

[‡]leng@sinap.ac.cn

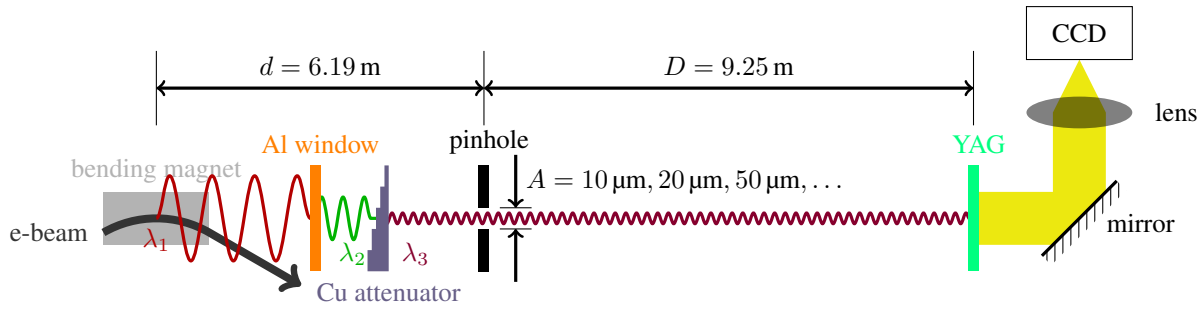


Figure 1: The layout of the X-ray pinhole camera system.

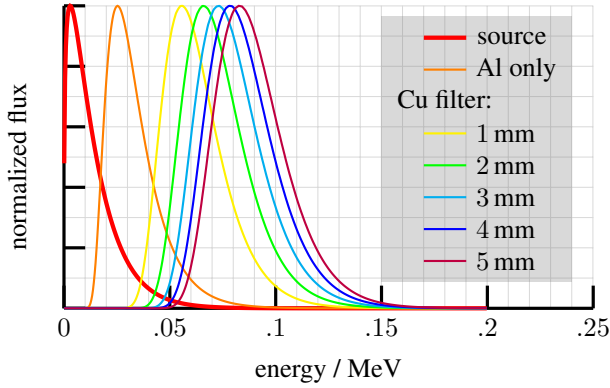


Figure 2: Normalized spectra of the synchrotron radiation after various filters.

CALIBRATION EXPERIMENT

Calibration Scheme

The angular distribution of radiation for relativistic particles can be expressed as [5]:

$$\frac{dP}{d\Omega} \simeq \frac{2}{\pi} \frac{e^2}{c^3} \gamma^6 \frac{|\dot{\mathbf{v}}|^2}{(1 + \gamma^2 \theta^2)^3} \left[1 - \frac{4\gamma^2 \theta^2 \cos^2 \phi}{(1 + \gamma^2 \theta^2)^2} \right]. \quad (5)$$

The above formula can be transformed to the Cartesian coordinate by using the following relation:

$$\tan \phi = \frac{y}{x},$$

$$\theta \simeq \tan \theta = \frac{\sqrt{x^2 + y^2}}{D + d}.$$

Then the vertical distribution can be derived by integrating the density function over x :

$$f(y) = \frac{dP}{dy} \simeq \frac{e^2 \gamma^5 |\dot{\mathbf{v}}|^2}{c^3} \frac{7(D + d)^8 + 12(D + d)^6 \gamma^2 y^2}{16((D + d)^2 + \gamma^2 y^2)^{7/2}}. \quad (6)$$

The beam energy of SSRF is $E = \gamma mc^2 = 3.5 \text{ GeV}$, and $D + d = 6.19 \text{ m} + 9.25 \text{ m} = 15.44 \text{ m}$. So the normalized density function is completely specified. The spatial range of the CCD is close to 1 mm, so it might not be precise enough to roughly assume the distribution is uniform (as shown in Fig. 3).

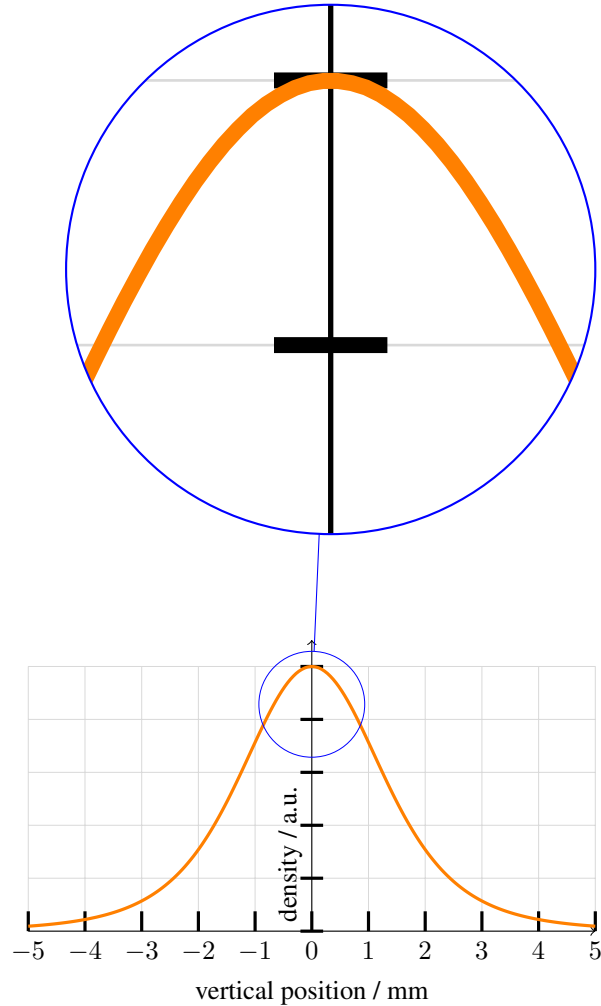


Figure 3: Vertical distribution of the synchrotron radiation reached the YAG screen.

It is theoretically easy to get the PSF of the imaging system by removing the pinhole component and letting the distributed X-ray pass through this system. The final image is the convolution of the distribution function and the PSF of the system: $f(y) * g(y)$. The difficulty in this scheme is that the resolution of the PSF obtained using deconvolution would be limited for the following reasons:

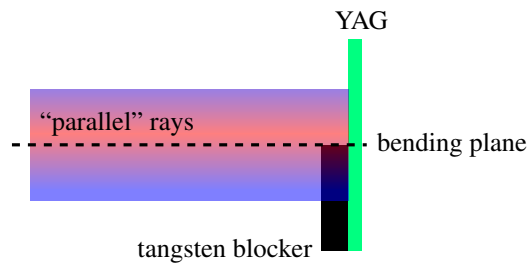


Figure 4: Setup for the PSF calibration of the imaging system.

- noise, including the quantization error of the CCD, has entered the resulting image that will not make the deconvolution reliable;
- the spacial resolution of the CCD is fixed and the samples is of the order of 100 in our device and the influences of the energy spread of the beam and the measurement error of the distance are hard to be estimated;
- although $f(y) * g(y)$ does have a distribution and has already been observed in the past experiments, the CCD is focusing on the bending plane with a relatively small interval and will not make use of the full dynamic range of the CCD.

In practice, a tungsten blocker was used to assist the measurement. The measurement took two steps: a reference image $(f * g)(y)$ was saved for future use, and a calibration image $((f \cdot u) * g)(y)$ was measured later when the blocker was placed just before the Ce:YAG screen as a step input (as shown in Fig. 4), and it would be true that the calibration image is the step response of the system only if the distribution $f(y)$ could be considered uniform or constant. By taking advantage of the fact that the derivative is a linear operator, the differential results of the images would be $f_1(y) = \frac{d}{dy}(f * g)(y) = ((\frac{d}{dy}f) * g)(y)$ and $f_2(y) = \frac{d}{dy}((f \cdot u) * g)(y) = (\frac{d}{dy}(f \cdot u)) * g)(y) = ((u \cdot \frac{d}{dy}f) * g)(y) + ((f \cdot \frac{d}{dy}u) * g)(y) = \frac{d}{dy}f(y > 0) * g(y) + ((f \cdot \delta) * g)(y) = ((\frac{d}{dy}f) * g)(y) / 2 + f(0) \cdot g(y) = f_1(y) / 2 + C \cdot g(y)$. The effect of the angular distribution on the output image thus can be eliminated.

Image Processing

The differential results of the reference image and the calibration image can be used to get the PSF directly, as described in the previous section. One can see that the coefficient $f(0)$ is trivial since only the r.m.s. width of the PSF will be used in Eq. (2). Furthermore, not only the angular distribution of the synchrotron radiation has been normalized, the noise—like the refraction in the Al window or the Cu filter that can change the distribution of the X-ray—entered the light can also be wiped out as long as it's symmetric about the bending plane.

The only inconvenient part is that a simple difference operation on the raw image will cause the r.m.s. of the

noise enlarged by $\sqrt{2}$ that can lead to a poorer resolution. To improve the computational accuracy, the images were “smoothed” by fitting a moving window with polynomials of degree n and the differential results were calculated by using the coefficients of the polynomials. The upper bound of the error was determined by the remainder of the n th-degree Taylor polynomial of the PSF. After the PSF was calculated, the r.m.s. size can be easily calculated by simply using the definition: $\sigma^2 = E[y^2] - E[y]^2$ where $E[F(y)] = \sum F(y_i)g(y_i)$.

CONCLUSIONS

The X-ray pinhole camera system used a simple design that can move the attenuator, the pinhole array and the imaging system independently to meet various needs.

The spectra of the synchrotron radiation were first simulated for each stair of the Cu attenuator which will give us a rough idea of choosing the optimized pinhole size and the corresponding PSF of the pinhole.

The analytic PSFs of the pinhole and the basic idea of calibrating the PSF of the whole imaging system based on the synchrotron radiation were adopted from [1]. An estimate of the power distribution of the radiation has shown than the implicit assumption of the uniform distribution in [1] was considered not suitable in SSRF. Thus, a further study was made to normalize the angular distribution of the radiation.

A detailed table/database between the r.m.s. size of the entire system and all the independent variables, e.g., thickness/position of the attenuator, size of the aperture of the pinhole, gain of the CCD, is still in progress and an empirical formula will be derived hopefully.

REFERENCES

- [1] Cyrille Thomas, Guenther Rehm and Ian Martin, “X-ray pinhole camera resolution and emittance measurement,” *Physical Review Special Topics—Accelerators and Beams* **13**, 022805 (2010).
- [2] Guoqing Huang, Jie Chen, Zhichu Chen, Yongbin Leng And Kairong Ye, “X-ray pinhole camera system design for SSRF storage ring,” *Nuclear Techniques* **33**, 806–809 (2010).
- [3] P. Elleaume, C. Fortgang, C. Penel, and E. Tarazona, *J. Synchrotron Radiat.* **2**, 209 (1995).
- [4] G. Blasse and A. Bril, “A NEW PHOSPHOR FOR FLYING-SPOT CATHODE-RAY TUBES FOR COLOR TELEVISION: YELLOW-EMITTING $Y_3Al_5O_{12}-Ce^{3+}$,” *Applied Physics Letters*, **11**, 1967, 53-55, doi: <http://dx.doi.org/10.1063/1.1755025>.
- [5] John David Jackson, *Classical Electrodynamics*, third edition, John Wiley & Sons, Inc., 1998.